scientific reports

Check for updates

OPEN

Assessing blood flow in uterine fibroids using intravoxel incoherent motion imaging compared with dynamic contrast-enhanced MRI

Teija Sainio[1]✉, Jani Saunavaara[1], Gaber Komar[2], Antti Viitala[2], Saara Otonkoski[3], Kirsi Joronen[3], Antti Perheentupa[3] & Roberto Blanco Sequeiros[2]

To assess the utility of IVIM parameters in evaluating uterine fibroid blood flow compared to dynamic contrast-enhanced magnetic resonance imaging (DCE-MRI) derived blood flow. Sixteen premenopausal women with uterine fibroids were enrolled in this prospective study. Pelvic MRI scans were obtained for each subject, both with and without continuous intravenous infusion of oxytocin, known to decrease significantly uterine fibroid blood flow, to assess the changes in blood flow of uterine fibroids. IVIM and DCE analyses were conducted using separate dedicated software. The bi-exponential IVIM model was used to estimate perfusion fraction (f), pseudo-diffusion coefficient (D*), and diffusion coefficient (D). DCE blood flow values were derived via T1 perfusion deconvolution arithmetic, utilizing a first pass of an AIF curve. The correlation between the parameters were analyzed by Spearman's rank correlation analysis due to small sample size. Means of the parameters were compared with a nonparametric Wilcoxon sign rank method for each pair. Statistically significant positive correlations were found between perfusion fraction values and DCE blood flow values with oxytocin (Spearson's $\rho = 0.78$, $p = 0.0004$), and between fD* values and DCE blood flow values with oxytocin (Spearson's $\rho = 0.64$, $p = 0.0071$). Significant differences in blood flow were detected across most IVIM parameters: f, D*, and fD* ($p < 0.001$, $p = 0.0027$, and $p = 0.0002$, respectively) when comparing the values without oxytocin and with oxytocin. IVIM imaging shows promise for assessing blood flow in uterine fibroids.

Keywords IVIM, DCE, Blood flow, Perfusion, Uterine fibroid

Uterine fibroids are benign uterine smooth-muscle cell tumors also known as leiomyomas or myomas which are the most common tumors encountered in women affecting up to two out of every three women of premenopausal age[1,2]. One of the key factors influencing the clinical behavior and management of uterine fibroids is their vascularity, particularly blood flow. Quantifying blood flow in uterine fibroids is crucial for understanding their pathophysiology, predicting treatment response, and guiding therapeutic interventions[3–7].

Dynamic contrast-enhanced magnetic resonance imaging (DCE-MRI) has been the cornerstone for assessing tissue perfusion and blood flow in various pathological conditions, including uterine fibroids[5,6,8–11]. However, DCE-MRI has limitations, including the need for gadolinium-based contrast agents, potential renal toxicity, and the need for repeated injections, which may not be suitable for all patients[12–14].

In recent years, intravoxel incoherent motion (IVIM) MRI has emerged as a promising non-invasive imaging technique for assessing tissue perfusion and microvascular architecture[15–19]. IVIM imaging exploits the microscopic motion of water molecules within tissues to derive quantitative parameters reflecting tissue microcirculation, including perfusion fraction (f), pseudo-diffusion coefficient (D*), and the product of perfusion fraction and pseudo-diffusion coefficient (fD*)[20].

While several studies have investigated the utility of DCE-MRI in assessing blood flow in uterine fibroids, research on the potential of IVIM imaging for this purpose is limited. This study aims to fill this gap by evaluating the efficacy of IVIM imaging as an alternative or complementary tool to DCE-MRI for quantifying blood flow in uterine fibroids.

[1]Department of Medical Physics, Turku University Hospital and University of Turku, Kiinamyllynkatu 4-8, Turku 20521, Finland. [2]Department of Radiology, Turku University Hospital and University of Turku, Kiinamyllynkatu 4-8, Turku 20521, Finland. [3]Department of Obstetrics and Gynecology, Turku University Hospital and University of Turku, Kiinamyllynkatu 4-8, Turku 20521, Finland. ✉email: Teija.sainio@varha.fi

To achieve this, we conducted a comparative analysis of IVIM and DCE-MRI in assessing blood flow changes in uterine fibroids by using oxytocin infusion, which has been shown to decrease significantly the blood flow of the uterine fibroids[4]. We hypothesized that IVIM imaging would demonstrate comparable efficacy to DCE-MRI in assessing perfusion in uterine fibroids, offering potential advantages such as reduced reliance on contrast agents and improved patient safety. This research contributes to expanding our understanding of the role of IVIM imaging in gynecological imaging and may influence future clinical practice guidelines for evaluating uterine fibroids.

Materials and methods

Patients

This study was approved by the Ethics Committee of the Hospital District of Southwest Finland and the National Committee of Medical Research Ethics (Approval Number: T366/2017, dated January 25, 2018). This study was performed in accordance with the Declaration of Helsinki. Written informed consent for both MRI procedures and oxytocin administration was obtained from all participating patients.

Sixteen premenopausal women (mean age 38 ± 6 years, mean BMI 25 ± 4) with twenty-six fibroids were consecutive patients referred to the gynecological outpatient clinic for potential magnetic resonance guided high-intensity focused (MRgHIFU) treatment, representing a specific subgroup of fibroid patients. Inclusion criteria for this study were symptoms caused by fibroids, physical and mental health suitable for an MRI scan, and premenopausal status. Exclusion criteria included a known allergy to Syntocinon or any of its adjuvants, high blood pressure, an ischemic heart condition, long QT syndrome, or medication that prolongs the QT segment. Additionally, women with contraindications to MRI were excluded. Patient and fibroid characteristics are presented in Table 1. The dominant fibroid (mean diameter 62 ± 23 mm) was assessed for each woman, and no areas of degeneration, necrosis or hemorrhage were identified in any of the fibroids.

MRI protocol

All sixteen patients underwent scanning with the same MR scanner (Ingenia 3.0T, Philips, Best, The Netherlands). Women were positioned in a prone position during the MRI scan of the pelvis, utilizing a 32-channel torso coil. An extended scanning protocol was employed for each patient, with the MR imaging parameters outlined in Table 2.

Subsequently, another MRI scan was conducted, with a median interval of 58 days (range 4-207 days), utilizing the same imaging protocol under continuous intravenous infusion of oxytocin. A total of 40 IU of oxytocin (Syntocinon 8.3 ug/ml, Sigma-Tau Industrie Farmaceutiche Riunite S.p.A) diluted to 500 ml of 0.9% NaCl was administered at a rate of 5 ml/min, resulting in an oxytocin infusion rate of 0.4 IU/min. To perform the oxytocin administration during MRI scan, a volumetric infusion pump (Infusomat® Space, B Braun, Germany, Melsungen) was placed in an MRI-compatible docking station (SpaceStation® MRI, B Braun, Germany, Melsungen). The MRI scan began approximately 15 min after the initiation of the oxytocin infusion.

DCE

The MRI protocol included a dynamic contrast enhanced (DCE) T1-weighted sequence, with the parameters detailed in Table 2. A single dose (0.2 mL/kg) of contrast agent (Dotarem, Guebert, Roissy, France) was manually injected at a constant rate followed by 10 mL saline flush after the acquisition of the first five time frames of the dynamic scans. Analysis of the DCE-MRI data was conducted using NordicICE software v. 4.1.1 (NordicNeuroLab AS, Bergen, Norway).

Patient	Age (years)	BMI	Number of fibroids	Largest fibroid diameter (mm)	FIGO type
1	41	25	1	79	2–5
2	44	22	4	57	2
3	49	20	1	44	1
4	26	21	1	46	3
5	43	27	1	63	1
6	45	20	4	71	7
7	31	28	4	44	2–5
8	31	22	1	50	2
9	35	34	1	128	2–5
10	36	29	1	40	2
11	31	21	2	68	2–5
12	28	19	1	88	6
13	38	23	1	71	2–5
14	42	31	1	59	2–5
15	42	23	1	60	2–5
16	38	28	1	61	2–5

Table 1. Characteristics of the patients and the fibroids enrolled in this study.

Parameter	T2W TSE	T2W TSE	DWI	T1W TFE SPAIR	T1W TFE SPAIR	Dynamic CE-T1W TFE SPAIR	CE-T1W TFE SPAIR	CE-T1W TFE SPAIR
Imaging plane	Sagittal	Axial	Axial	Sagittal	Axial	Axial	Sagittal	Axial
Repetition time (ms)	4844	3845	3733	5.2	5.4	2.9	5.2	5.4
Echo time (ms)	95	80	83	2.6	2.6	1.3	2.6	2.6
Flip angle (°)	90	90	90	7	7	10	7	7
Number of slices	42	45	30	225	133	40	225	133
Number of dynamics	–	–	–	–	–	70	–	–
b-values	–	–	0, 50, 100, 200, 400, 600, 800	–	–	–	–	–
TSE/TFE/EPI factor	28	19	67	80	80	19	80	80
Slice thickness (mm)	3	4	5	3	3	6	3	3
Matrix size MxP	344 × 267	272 × 241	124 × 96	168 × 232	172 × 298	112 × 145	168 × 232	172 × 298
Field of view AP × FH × RL (mm)	240 × 240 × 138	300 × 198 × 300	288 × 150 × 375	250 × 345 × 338	255 × 200 × 448	270 × 120 × 349	250 × 345 × 338	255 × 200 × 448

Table 2. MR imaging parameters.

The arterial input function (AIF) was determined from the iliac artery by placing a circular region of interest (ROI) on the artery lumen. Blood flow (BF_{DCE}) values were calculated using a standard model-independent deconvolution technique through contrast bolus tracking[21]. Parametric blood flow values were derived via T1 perfusion deconvolution arithmetic, utilizing a first pass of an AIF curve. ROIs were delineated within three middle slices of the fibroid to include most of the fibroid to obtain averaged blood flow values.

IVIM

MRI protocol included a diffusion-weighted imaging (DWI) sequence, with the parameters detailed in Table 2. To mitigate breathing and movement artifacts, two saturation slabs were employed in the DWI scan, the slabs were positioned over the abdominal and dorsal fat regions. The DW images were acquired with b-values of 0, 50, 100, 200, 400, 600, and 800 s/mm^2. All IVIM parameter maps were reconstructed with Philips IntelliSpace Portal v11.1 (Philips medical systems Nederland B.V., Best, The Netherlands) by using a bi-exponential model and full fitting.

ROIs were delineated in the three middle slices of the fibroid to encompass the majority of the fibroid tissue while avoiding the partial volume effect caused by the large 5 mm voxels at tissue borders. This was achieved by positioning the ROI border a few millimeters inside the fibroid. The size of the ROI was adjusted based on the dimensions of the fibroid. Subsequently, the ROIs were replicated on all IVIM parameter maps within the same three sequential slices, and averaged values were derived from each IVIM parameter map.

Statistical analysis

Statistical analysis was performed using JMP Pro statistical software version 16.1.0 (SAS Institute Inc.). A p-value less than 0.05 was considered statistically significant.

The correlation between the parameters were analyzed by Spearman's rank correlation analysis due to small sample size. The confidence interval for the Spearman correlation coefficient was estimated using Fisher's z-transformation. Means of the parameters were compared with a nonparametric Wilcoxon sign rank method for each pair.

Results

Relationships between IVIM parameters and blood flow values

A statistically significant positive correlation was identified between perfusion fraction (f) values and blood flow (BF_{DCE}) values with oxytocin (Spearman's $\rho = 0.78$, p-value = 0.0004), along with a similar correlation between the product fD* values and blood flow (BF_{DCE}) values with oxytocin (Spearman's $\rho = 0.64$, p-value = 0.0071). All corresponding p-values and Spearman's rank correlation coefficients (ρ) are presented in Table 3.

Difference between each parameter without oxytocin and with oxytocin

A statistically significant difference in blood flow (BF_{DCE}) values was detected between scans conducted without oxytocin and those with oxytocin infusion ($p < 0.0001$). Furthermore, the same statistically significant difference could be detected across almost all IVIM parameters: f, D*, and fD* ($p < 0.001$, $p = 0.0027$, and $p = 0.0002$, respectively). All median values and p-values are shown in Table 4 and corresponding box-whisker plots are shown in Fig. 1. An example of images with and without oxytocin are shown in Fig. 2.

Discussion

While several studies[5,6,9,10] have investigated the utility of the DCE-MRI for assessing blood flow in uterine fibroids, the potential of IVIM imaging in this context remains largely unexplored. Previous studies[22,23] have demonstrated that there is a non-mono-exponential dependence between the signal decay and the b-value in uterine fibroids. This finding suggests that IVIM imaging could offer valuable insights into the vascular properties

IVIM parameter	DCE parameter	Spearman's coefficient (95% confidence interval)	*p*-value
D	BF	0.16 (−0.37, 0.61)	0.5495
D oxytocin	BF oxytocin	0.11 (−0.41, 0.58)	0.6803
f	BF	0.15 (−0.37, 0.60)	0.5792
f oxytocin	BF oxytocin	0.78 (0.40, 0.93)	0.0004
D*	BF	−0.45 (−0.78, 0.09)	0.0803
D* oxytocin	BF oxytocin	0.39 (−0.15, 0.75)	0.1373
fxD*	BF	−0.46 (−0.79, 0.08)	0.0759
fxD* oxytocin	BF oxytocin	0.64 (0.17, 0.88)	0.0071

Table 3. Correlation coefficients with 95% confidence intervals and p-values between IVIM parameters and blood flow values.

Parameter	Without oxytocin	With oxytocin	*p*-value
BF_{DCE} [ml/100 g/min]	38.6 (21.1–101.3)	3.6 (2.0–14.2)	0.0001
D [$\times 10^{-6}$ mm^2/s]	1083.3 (997.5–1236.7)	900.0 (769.2–1263.3)	0.0546
F	0.24 (0.14–0.26)	0.08 (0.07–0.15)	< 0.0001
D* [$\times 10^{-6}$ mm^2/s]	31,980 (22423–38746)	12,472 (7332–26811)	0.0027
f × D* [$\times 10^{-6}$ mm^2/s]	7569 (5469–10525)	1165 (486–8912)	0.0002

Table 4. Median values and p-values for each parameter without oxytocin and with oxytocin.

of uterine fibroids. One of the key advantages of IVIM imaging over DCE-MRI is its non-reliance on exogenous contrast agents. While DCE-MRI necessitates the administration of gadolinium-based contrast agents, which may pose risks such as renal toxicity and allergic reactions, IVIM imaging eliminates the need for contrast administration[12–14]. This eliminates potential safety concerns associated with contrast agents, making IVIM imaging a safer and more patient-friendly option. Furthermore, IVIM imaging offers practical advantages in terms of image acquisition and post-processing. Unlike DCE-MRI, which requires a relatively long acquisition time (approximately 5 min) and complex manual post-processing for quantitative analysis, IVIM imaging can be performed using a standard diffusion-weighted imaging sequence with a relatively short acquisition time (less than 5 min) and automatic post-processing. This reduction in scan time and post-processing could not only enhance patient comfort and throughput in clinical settings but also increase the efficiency of radiologists.

Our findings revealed a statistically significant positive correlation between perfusion fraction (f) and blood flow (BF_{DCE}) in uterine fibroids. Additionally, the IVIM parameters f, D*, and fD* were able to differentiate blood flow changes in uterine fibroids. These results suggest that IVIM imaging effectively captures variations in fibroid perfusion, providing valuable insights into the hemodynamic characteristics of fibroid tissues. Our result is in line with recently published work by Slotman et al.[24], where they studied perfusion changes in uterine fibroids during MR-guided high intensity focused ultrasound (MRgHIFU) treatment. Moreover, these results could indicate that especially perfusion fraction maps could be utilized in clinical routine to evaluate perfusion in uterine fibroids. However, it should be noted that the previous studies[18,25–27] have reported less conclusive results of the correlation between the perfusion fraction and DCE blood volume in other anatomical regions such as brain and liver. This discrepancy could indicate that the robustness and reliability of IVIM analysis results may vary depending on the anatomical region or other factors.

We also observed that the median diffusion coefficient decreases with the effect of oxytocin as perfusion decreases. However, this change was not statistically significant in this dataset ($p = 0.0546$). The decrease in the diffusion coefficient may be attributed to oxytocin causing contraction of the uterine fibroid smooth muscle, thereby restricting diffusion in the tissue. Further investigation into this phenomenon is warranted in the future.

Despite these promising advantages and results, it is important to acknowledge the limitations of IVIM imaging for assessing blood flow in uterine fibroids. IVIM imaging may be susceptible to confounding factors such as motion artifacts and tissue heterogeneity, which can affect the accuracy and reproducibility of perfusion measurements[20,28]. Additionally, further validation studies are needed to confirm the reliability and clinical utility of IVIM imaging in comparison to DCE-MRI.

One of the limitations of this study is the small number of patients included in this study, which may limit the generalizability of our findings. A larger sample size would enhance the statistical power and robustness of the results. However, even with this small dataset, statistically significant results were observed. Second, oxytocin could induce T2 relaxation time changes in uterine fibroids that might affect the measured IVIM parameters[29]. However, this study aimed to evaluate the utility of IVIM imaging in assessing blood flow in clinical routine rather than measuring quantitative values. Thirdly, the study was conducted at a single center, which may introduce bias and limit the external validity of the findings. Multi-center studies involving diverse patient populations are needed to confirm the reproducibility of our results. Fourth, uterine fibroids are heterogeneous tumors with variable sizes, locations, and vascular patterns. Our study did not stratify participants based on fibroid characteristics, potentially overlooking important variations in blood flow dynamics among different

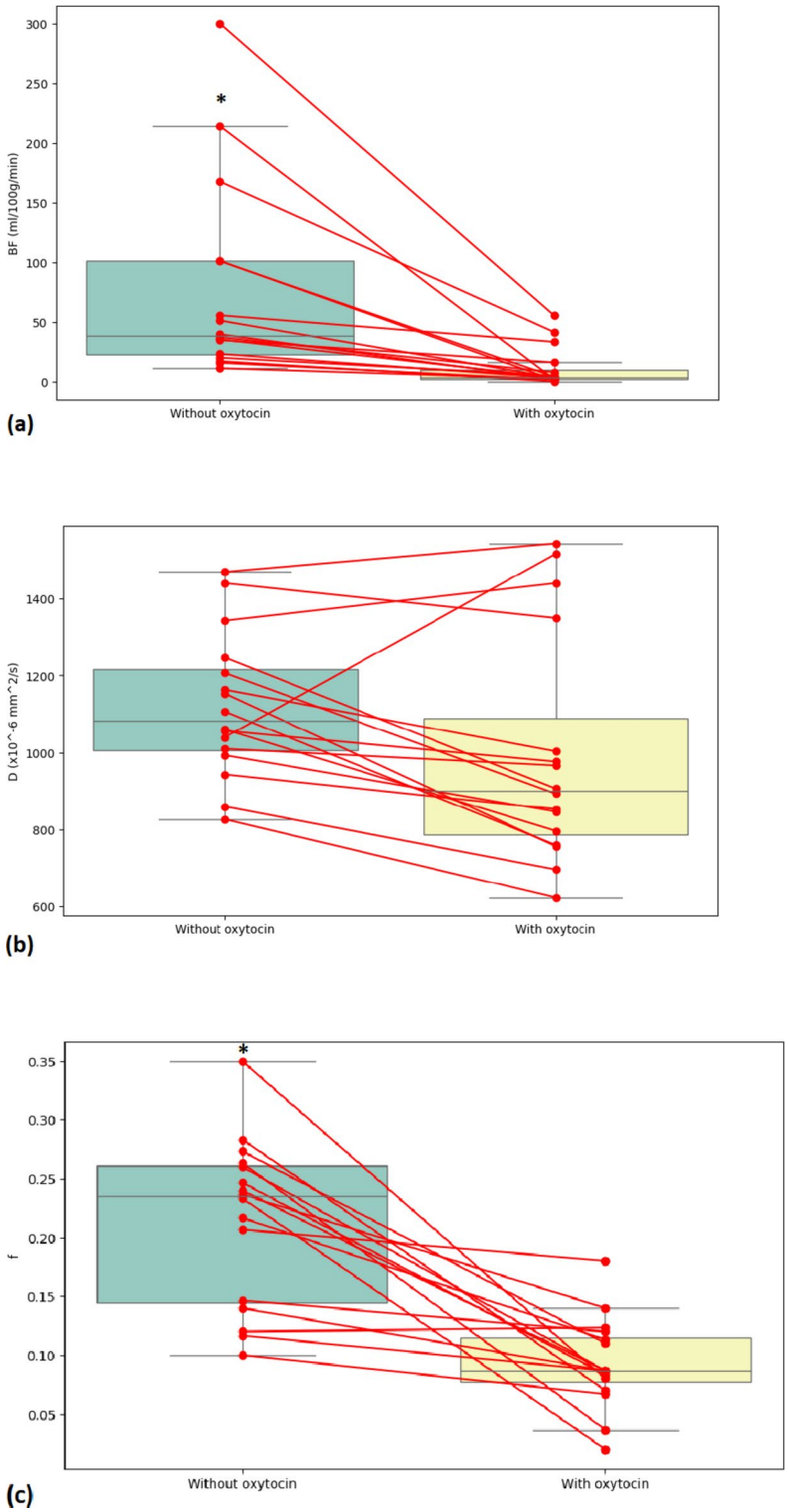

Fig. 1. Box–Whisker plots with connecting lines for each patient presenting values without oxytocin and with oxytocin for (**a**) DCE blood flow (**b**) diffusion coefficient, (**c**) perfusion fraction, (**d**) pseudo-diffusion coefficient, and (**e**) product of perfusion fraction and pseudo-diffusion coefficient (*p-value < 0.05).

fibroid subtypes. Fifth, MR scanning sessions were not performed consecutively to allow the contrast agent to clear from the body before the next scan. This may have caused the experimental setup to differ slightly when comparing perfusions, potentially leading to other factors, such as changes in the uterine fibroid and variability in the calibrations of the MR scanner, affecting the perfusion changes. However, we did not observe any significant changes in the uterine fibroids between the scans. Sixth, while our study focused on IVIM

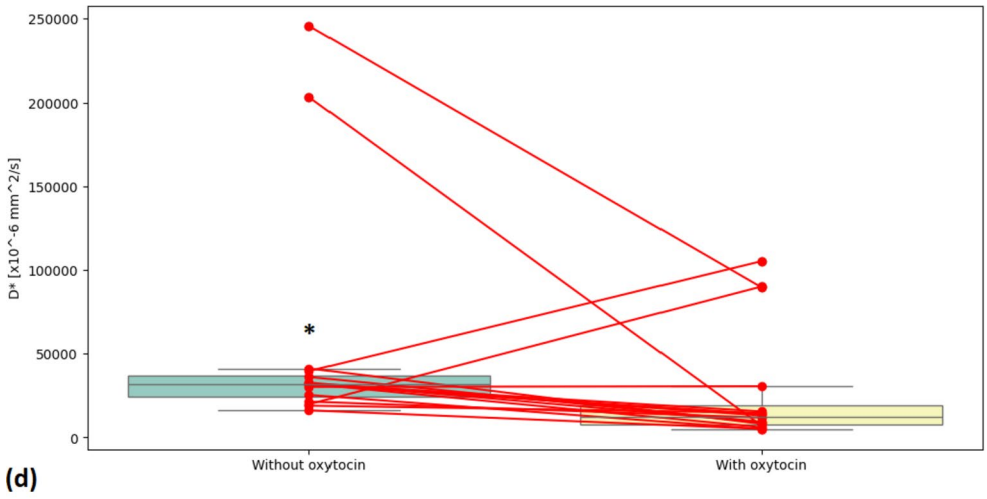

(d)

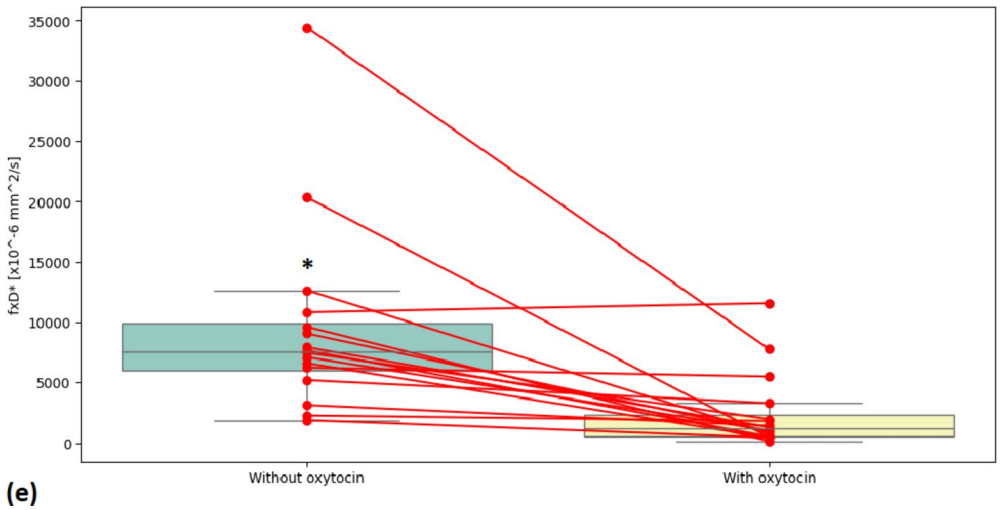

(e)

Figure 1. (continued)

imaging, we did not directly compare its performance with that of dynamic contrast-enhanced MRI (DCE-MRI) for assessing blood flow in uterine fibroids. Future studies should conduct head-to-head comparisons between IVIM and DCE-MRI to evaluate their relative strengths and limitations. Additionally, attention should be paid to diffusion-weighted imaging parameters, as they can affect the IVIM results, especially the choice of the b-values can exert an impact on the calculated IVIM values[20]. Addressing these limitations through larger, multi-center studies with longitudinal designs and comprehensive comparative analyses would strengthen the evidence base regarding the utility of IVIM imaging for evaluating blood flow in uterine fibroids.

In conclusion, our study provides preliminary evidence supporting the potential utility of IVIM imaging as an alternative method for quantifying blood flow in uterine fibroids. By offering a safer, more accessible, and more straightforward approach to assessing fibroid perfusion, IVIM imaging holds promise as a valuable tool in the clinical evaluation and management of uterine fibroids. Further research is warranted to validate these findings and to explore the broader applicability of IVIM imaging in gynecological and oncological imaging.

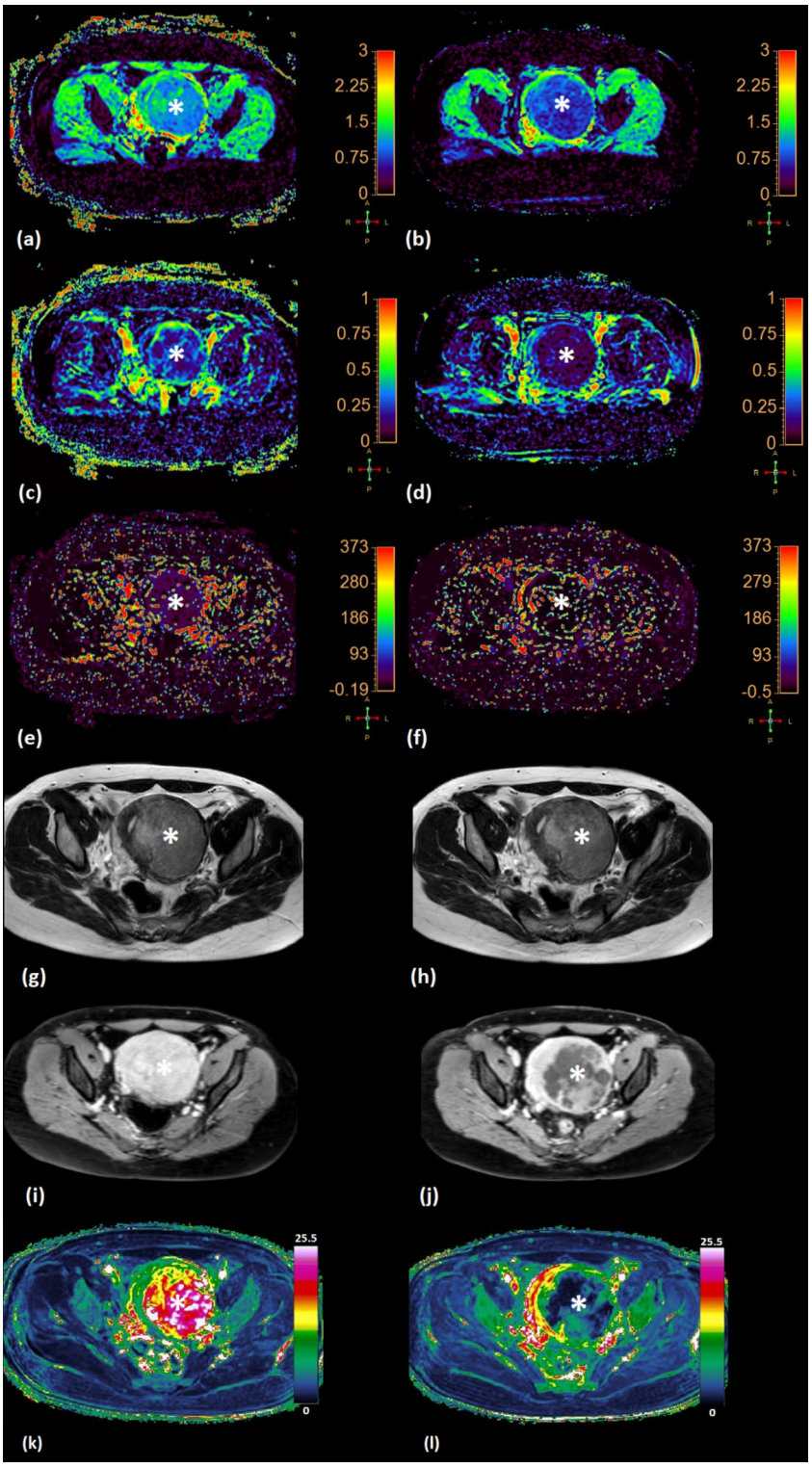

Fig. 2. Example of diffusion coefficient map [$\times 10^{-3}$ mm^2/s] (**a**) without oxytocin and (**b**) with oxytocin, perfusion fraction map (**c**) without oxytocin and (**d**) with oxytocin, and pseudo-diffusion coefficient map [$\times 10^{-3}$ mm^2/s] (**e**) without oxytocin and (**f**) with oxytocin, T2-weighted image (**g**) without oxytocin and (**h**) with oxytocin, contrast enhanced T1-weighted image (**i**) without oxytocin and (**j**) with oxytocin, parametric DCE blood flow map (**k**) without oxytocin and (**l**) with oxytocin. Uterine fibroid is marked with asterisk sign.

Data availability

The datasets used and/or analysed during the current study available from the corresponding author on reasonable request.

Received: 14 August 2024; Accepted: 17 December 2024
Published online: 23 January 2025

References

1. Cramer, S. F. & Patel, A. The frequency of uterine leiomyomas, *Am. J. Clin. Pathol.*, vol. 94, no. 4 SUPPL. 1, pp. 435–438, (1990).
2. Stewart, E. A. Uterine fibroids. *Lancet* **357** (9252), 293–298. https://doi.org/10.1016/S0140-6736(00)03622-9 (2001).
3. Malone, C. D. et al. Pelvic blood Flow predicts fibroid volume and Embolic required for uterine fibroid embolization: a pilot study with 4D Flow MR Angiography. *Am. J. Roentgenol.* **210** (1), 189–200. https://doi.org/10.2214/AJR.17.18127 (Jan. 2018).
4. Otonkoski, S. et al. Oxytocin selectively reduces blood flow in uterine fibroids without an effect on myometrial blood flow: a dynamic contrast enhanced MRI evaluation. *Int. J. Hyperth.* **37** (1), 1293–1300. https://doi.org/10.1080/02656736.2020.1846792 (2020).
5. Wei, C. et al. The predictive value of quantitative DCE metrics for immediate therapeutic response of high-intensity focused ultrasound ablation (HIFU) of symptomatic uterine fibroids, *Abdom. Radiol.*, vol. 43, no. 8, pp. 2169–2175, Aug. doi: (2018). https://doi.org/10.1007/s00261-017-1426-7
6. Kim, Y. S. et al. Oct., Dynamic Contrast-Enhanced Magnetic Resonance Imaging Predicts Immediate Therapeutic Response of Magnetic Resonance-Guided High-Intensity Focused Ultrasound Ablation of Symptomatic Uterine Fibroids, *Invest. Radiol.*, vol. 46, no. 10, pp. 639–647, doi: (2011). https://doi.org/10.1097/RLI.0b013e318220785c
7. Iavazzo, C., Mamais, I. & Gkegkes, I. D. Use of misoprostol in myomectomy: a systematic review and meta-analysis, *Arch. Gynecol. Obstet.*, vol. 292, no. 6, pp. 1185–1191, Dec. doi: (2015). https://doi.org/10.1007/s00404-015-3779-x
8. Tofts, P. S. & Parker, G. J. M. DCE-MRI: Acquisition and analysis techniques, in Clinical Perfusion MRI: Techniques and Applications, (eds Barker, P., Golay, X. & Zaharchuk, G.) Cambridge University Press, 58–74. (2013).
9. Kim, Y. S. et al. Uterine fibroids: semiquantitative perfusion MR imaging parameters associated with the intraprocedural and immediate postprocedural treatment efficiencies of MR imaging-guided high-intensity focused ultrasound ablation. *Radiology* **273** (2), 462–471. https://doi.org/10.1148/radiol.14132719 (2014).
10. Li, C. et al. Magnetic resonance-guided high-intensity focused ultrasound of uterine fibroids: whole-tumor quantitative perfusion for prediction of immediate ablation response. *Acta Radiol.* **61** (8), 1125–1133. https://doi.org/10.1177/0284185119891692 (2020).
11. Yankeelov, T. & Gore, J. Dynamic Contrast Enhanced Magnetic Resonance Imaging in Oncology:theory, Data Acquisition,Analysis, and examples. *Curr. Med. Imaging Rev.* **3** (2), 91–107. https://doi.org/10.2174/157340507780619179 (May 2009).
12. Rogosnitzky, M. & Branch, S. Gadolinium-based contrast agent toxicity: a review of known and proposed mechanisms, *BioMetals*, vol. 29, no. 3, pp. 1–12, doi: (2016). https://doi.org/10.1007/s10534-016-9931-7
13. Ersoy, H. & Rybicki, F. J. Biochemical safety profiles of gadolinium-based extracellular contrast agents and nephrogenic systemic fibrosis. *J. Magn. Reson. Imaging.* **26** (5), 1190–1197. https://doi.org/10.1002/jmri.21135 (2007).
14. Thomsen, H. S., Morcos, S. K. & Dawson, P. Is there a causal relation between the administration of gadolinium based contrast media and the development of nephrogenic systemic fibrosis (NSF)? *Clin. Radiol.* **61** (11), 905–906. https://doi.org/10.1016/j.crad.2006.09.003 (2006).
15. Döpfert, J., Lemke, A., Weidner, A. & Schad, L. R. Investigation of prostate cancer using diffusion-weighted intravoxel incoherent motion imaging. *Magn. Reson. Imaging.* **29** (8), 1053–1058. https://doi.org/10.1016/j.mri.2011.06.001 (2011).
16. Wirestam, R. et al. Perfusion-related parameters in intravoxel incoherent motion MR imaging compared with CBV and CBF measured by dynamic susceptibility-contrast MR technique. *Acta Radiol.* **42** (2), 123–128. https://doi.org/10.1080/028418501127346459 (2001).
17. Kooreman, E. S. et al. Longitudinal Correlations Between Intravoxel Incoherent Motion (IVIM) and Dynamic Contrast-Enhanced (DCE) MRI During Radiotherapy in Prostate Cancer Patients, *Front. Oncol.*, vol. 12, no. June, pp. 1–10, doi: (2022). https://doi.org/10.3389/fonc.2022.897130
18. Fujima, N. et al. Intravoxel incoherent motion diffusion-weighted imaging in head and neck squamous cell carcinoma: Assessment of perfusion-related parameters compared to dynamic contrast-enhanced MRI. *Magn. Reson. Imaging.* **32** (10), 1206–1213. https://doi.org/10.1016/j.mri.2014.08.009 (2014).
19. Lei, J. et al. Preliminary study of IVIM-DWI and DCE-MRI in early diagnosis of esophageal cancer. *Eur. Rev. Med. Pharmacol. Sci.* **19** (18), 3345–3350 (2015).
20. Bihan, D. L. What can we see with IVIM MRI? *Neuroimage*, vol. 187, no. September pp. 56–67, 2019, doi: (2017). https://doi.org/10.1016/j.neuroimage.2017.12.062
21. Østergaard, L., Weisskoff, R. M., Chesler, D. A., Gyldensted, G. & Rosen, B. R. High resolution measurement of cerebral blood flow using intravascular tracer bolus passages. Part I: Mathematical approach and statistical analysis. *Magn. Reson. Med.* **36** (5), 715–725. https://doi.org/10.1002/mrm.1910360510 (1996).
22. Ikink, M. E. et al. Diffusion-weighted magnetic resonance imaging using different b-value combinations for the evaluation of treatment results after volumetric MR-guided high-intensity focused ultrasound ablation of uterine fibroids. *Eur. Radiol.* **24** (9), 2118–2127. https://doi.org/10.1007/s00330-014-3274-y (2014).
23. Sainio, T. et al. Feasibility of apparent diffusion coefficient in predicting the technical outcome of MR-guided high-intensity focused ultrasound treatment of uterine fibroids–a comparison with the Funaki classification. *Int. J. Hyperth.* **38** (1), 85–94. https://doi.org/10.1080/02656736.2021.1874545 (2021).
24. Slotman, D. J. et al. Dec., Intravoxel incoherent motion (IVIM)-derived perfusion fraction mapping for the visual evaluation of MR-guided high intensity focused ultrasound (MR-HIFU) ablation of uterine fibroids, *Int. J. Hyperth.*, vol. 41, no. 1, doi: (2024). https://doi.org/10.1080/02656736.2024.2321980
25. Lee, E. Y. P. et al. Aug., Relationship between intravoxel incoherent motion diffusion-weighted MRI and dynamic contrast-enhanced MRI in tissue perfusion of cervical cancers, *J. Magn. Reson. Imaging*, vol. 42, no. 2, pp. 454–459, doi: (2015). https://doi.org/10.1002/jmri.24808
26. Chandarana, H. et al. Diffusion-weighted intravoxel incoherent motion imaging of renal tumors with histopathologic correlation. *Invest. Radiol.* **47** (12), 688–696. https://doi.org/10.1097/RLI.0b013e31826a0a49 (Dec. 2012).
27. Marzi, S., Stefanetti, L., Sperati, F. & Anelli, V. Relationship between diffusion parameters derived from intravoxel incoherent motion MRI and perfusion measured by dynamic contrast-enhanced MRI of soft tissue tumors. *NMR Biomed.* **29** (1), 6–14. https://doi.org/10.1002/nbm.3446 (Jan. 2016).
28. Federau, C. Measuring perfusion: Intravoxel Incoherent Motion MR Imaging. *Magn. Reson. Imaging Clin. N Am.* **29** (2), 233–242. https://doi.org/10.1016/j.mric.2021.01.003 (May 2021).
29. Ma, F. Z. & Wáng, Y. X. J. T2 relaxation time elongation of hepatocellular carcinoma relative to native liver tissue leads to an underestimation of perfusion fraction measured by standard intravoxel incoherent motion magnetic resonance imaging. *Quant. Imaging Med. Surg.* **14** (1), 1316–1322. https://doi.org/10.21037/qims-23-1437 (Jan. 2024).

Author contributions

T.S. wrote the main manuscript text and prepared all the figures and tables. All authors reviewed the manuscript.J.S. made substantial contributions to the acquisition, analysis, or interpretation of data.All authors made substantial contributions to the design of the work.All authors revised the work critically for important intellectual content, approved the version to be published, and agree to be accountable for all aspects of the work in ensuring that questions related to the accuracy or integrity of any part of the work are appropriately investigated and resolved.

Declarations

Compliance with ethical standards

This study was approved by the Ethics Committee of the Hospital District of Southwest Finland and the National Committee of Medical Research Ethics (Approval Number: T366/2017, dated January 25, 2018). This study was performed in accordance with the Declaration of Helsinki.

Competing interests

The authors declare no competing interests.

Consent to participate and publish

Written informed consent was obtained from all individual participants included in the study.

Additional information

Correspondence and requests for materials should be addressed to T.S.

Reprints and permissions information is available at www.nature.com/reprints.

Publisher's note Springer Nature remains neutral with regard to jurisdictional claims in published maps and institutional affiliations.